Available online at www.sciencedirect.com
ScienceDirect
International Journal of Sediment Research 25 (2010) 258-270
INTERNATIONAL JOURNAL OF SEDIMENT RESEARCH
www.elsevier.com/locate/ijsrc

Experimental investigation of flow pattern and sediment deposition in rectangular shallow reservoirs

Matthieu DUFRESNE[1], Benjamin J. DEWALS[2], Sébastien ERPICUM[3], Pierre ARCHAMBEAU[4], and Michel PIROTTON[5]

Abstract

This paper reports the experimental investigation of flow pattern, preferential regions of deposition and trap efficiency as a function of the length of rectangular shallow reservoirs. Four flow patterns were identified (from longer to shorter reservoirs): an asymmetric flow with two reattachment points, an asymmetric flow with one reattachment point, an unstable flow, and a symmetric flow without any reattachment point. Using dye visualizations, the median value and the temporal variability of the reattachment lengths were precisely measured for the asymmetric flows. For each stable flow, sediment tests with plastic particles were carried out. The regions of deposition on the bed of the reservoir were clearly a function of the flow pattern. The transition from an asymmetric flow pattern to a symmetric flow pattern was responsible for an abrupt decrease of the trap efficiency; a number of regression laws were discussed to take it into account.

Key Words: Deposition, Flow patterns, Reservoirs, Sediment, Shallow water

1 Introduction

Tanks, basins, ponds, lagoons (called reservoirs below) are commonly used in hydraulic engineering. Because of generally quiescent conditions, these works are conducive to the settling of particles. Therefore, reservoirs must be carefully designed according to the role they will play. For example, sedimentation must be maximized in settling basins (stormwater treatment, protection of irrigation or hydro-electric power structures, etc.) whereas it must be minimized in storage facilities (irrigation, hydro-electric power generation, flood control, etc.).

The prediction of deposition as a function of the geometry of the reservoir, the hydraulic conditions and the sediment characteristics is still a great challenge. While empirical and semi-empirical methods have been developed for the last sixty years to determine the amount of deposits (see for example Jothiprakash

[1] Dr., Postdoctoral researcher, University of Liège (ULg), ArGEnCO department, MS²F sector, Hydrology, applied hydrodynamics and hydraulic constructions (HACH), Chemin des chevreuils, 1, bât B52/3, étage +1, 4000 Liège, Belgium. E-mail: matthieu.dufresne@free.fr, hach@ulg.ac.be

[2] Dr., Postdoctoral researcher of Belgian fund for scientific research (F.R.S.-FNRS), University of Liège (ULg), ArGEnCO department, MS²F sector, Hydrology, applied hydrodynamics and hydraulic constructions (HACH), Chemin des chevreuils, 1, bât B52/3, étage +1, 4000 Liège, Belgium.

[3] Dr., Laboratory manager, University of Liège (ULg), ArGEnCO department, MS²F sector, Hydrology, applied hydrodynamics and hydraulic constructions (HACH), Chemin des chevreuils, 1, bât B52/3, étage +1, 4000 Liège, Belgium.

[4] Dr., Research scientist, University of Liège (ULg), ArGEnCO department, MS²F sector, Hydrology, applied hydrodynamics and hydraulic constructions (HACH), Chemin des chevreuils, 1, bât B52/3, étage +1, 4000 Liège, Belgium.

[5] Prof., University of Liège (ULg), ArGEnCO department, MS²F sector, Hydrology, applied hydrodynamics and hydraulic constructions (HACH), Chemin des chevreuils, 1, bât B52/3, étage +1, 4000 Liège, Belgium.

Note: The original manuscript of this paper was received in Nov. 2009. The revised version was received in April 2010. Discussion open until Sept. 2011.

and Garg, 2008 for reservoirs, Garde et al., 1990, Ranga Raju et al., 1999 for basins; Kowalski et al., 1999 for combined sewer detention tanks; Luyckx et al., 1999 for high side weir overflows), they cannot determine their spatial distribution, which is required to well define the sediment removal strategy. To get this information, the knowledge of the flow pattern is a prerequisite. It is also questionable whether the relative imprecision of these methods is not because they express the trap efficiency of the reservoir (the ratio of the deposited mass to the incoming mass) without taking into account the flow pattern.

Saul and Ellis (1992) highlighted that complex flow patterns take place in rectangular storage tanks and that the flow pattern governs the sediment transport processes. Stovin and Saul (1994) carried out experiments in a 2.00 m long and 0.97 m wide storage tank. The circular inlet and outlet were respectively 0.19 m and 0.15 m in diameter. The water depth was about 0.20 m (the geometry was quasi bi-dimensional). The velocity in the inflow pipe was 0.56 m/s. Crushed olive stone was used as the model sediment (median grain size ≈ 0.050 mm, density ≈ 1,500 kg/m^3). The writers showed that the flow field was characterised by a large clockwise circulation and a small counter clockwise circulation in the upstream left corner of the tank (asymmetric flow pattern); deposits were located in three preferential regions: in both upstream corners of the tank and in the core of the large circulation zone. Varying the inflow velocity (in the range ≈ 0.1–0.7 m/s), Stovin and Saul (1996) proposed a linear relationship between the percentage of the bed that is covered by deposits and the trap efficiency.

Kantoush et al. investigated the influence of the geometry of shallow reservoirs on flow patterns and sedimentation by suspended sediments (Kantoush, 2008, Kantoush et al., 2008). His benchmark case was a 0.20 m high water flow entering a 6.00 m long and 4.00 m wide reservoir by a 0.25 m wide channel at a velocity of 0.14 m/s. In this situation the main flow was deflected on the right wall, leading to the formation of a large counter clockwise circulation zone in the whole structure and a small clockwise circulation zone in the right inlet corner (the jet may also be deflected on the left wall, depending on the experiment). Similar patterns were observed when decreasing the breadth of the reservoir (3.00 m, 2.00 m, 1.00 m and 0.50 m for which the flow was fully reattached in the downstream zone of the reservoir). Asymmetry disappeared when decreasing the length of the reservoir (5.00 m, 4.00 m, and 3.00 m). For these geometries, the jet was not deflected at entrance in the reservoir, leading to the formation of two large symmetric circulation zones. The writer used crushed walnut shells (median grain size ≈ 0.050 mm, density ≈ 1,500 kg/m^3) to study morphological evolution. Nevertheless, the flow pattern was not steady during sediment tests, probably because of the large amount of deposits near the inlet of the reservoir (these deposits led to change the direction of the jet entering the basin during experiments).

A number of experimental studies were conducted in more complex geometries. Modifying the basic chamber configuration described above, Stovin (1996) highlighted some effects of the gradient benching and the length to breadth ratio on sediment distribution. Dufresne et al. (2009) showed that flow and sediment distribution became quasi-symmetric when increasing the water level above the top of the inlet pipe. The influence of columns and obstacles (a wall located in front of the inlet) on sediment deposition was also investigated (Dufresne, 2008).

This study focuses on rectangular shallow reservoirs, as illustrated in Fig. 1. Here, L = length of the reservoir; B = breadth of the reservoir; b = breadth of the inlet and outlet channels; ΔB = lateral expansion; h = water depth; and U = inflow velocity. The aim of this work is firstly to investigate the preferential regions of deposition for the main flow patterns that can take place in rectangular shallow reservoirs; secondly, to study the influence of the flow pattern on the trap efficiency.

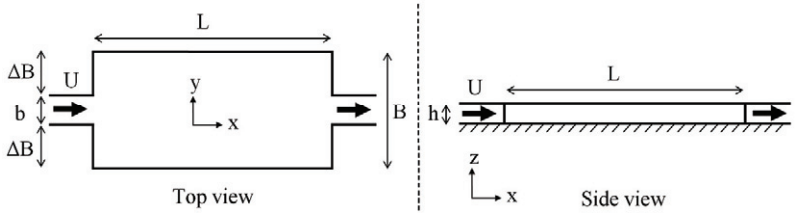

Fig. 1 Schemes of a rectangular shallow reservoir

2 Experimental investigation

2.1 Experimental set-up

The experiments were carried out at the engineering hydraulics laboratory of the University of Liège, Belgium. The experimental set-up diagrammatically shown in Fig. 1 consisted of a 10.40 m long and 0.985 m wide glass channel in which blocks can be arranged to build different geometries of rectangular reservoirs. The base of the flume was horizontal.

The flow entered the channel from a stilling basin through a porous screen in order to prevent fluctuations in water level and make the velocity field uniform. The flow was then contracted to the desired breadth of the inlet channel (b) in a converging section with circular shape; the inlet section of the reservoir (with straight parallel walls) was 2.00 m long. At the entrance of the reservoir, the flow suddenly expanded to the breadth of the reservoir (B). At the exit of the reservoir, the flow suddenly contracted to the outlet channel breadth (b). The outlet channel was 1.00 m long; its downstream boundary corresponded to a gate (to control the water level) and a waterfall. All the surfaces were made of glass, except the two parallel walls of the inlet and outlet channels (PVC) and the converging section (metallic sheets). In this study, the lateral expansion equaled 0.350 m. Three lengths were investigated: 1.80, 2.20 and 7.00 m; they were chosen after trial and error so that different flow patterns could be observed (symmetric flow, asymmetric flow with one reattachment point and asymmetric flow with two reattachment points).

The volumetric flow rate was measured with an electromagnetic flowmeter upstream of the flume; it was also measured with a triangular weir in the water collection channel downstream of the waterfall in order to enhance accuracy on small values. Water depth in the reservoir was measured with a level meter in the middle of the breadth 0.10 m downstream of the entrance of the reservoir and 0.10 m upstream of the exit of the reservoir. The maximum difference between the two values was 0.002 m. Therefore only the upstream value is reported hereafter.

2.2 Sediment

Granular plastic (Styrolux 656 C) was chosen as the model sediment. The particles were elliptical cylinders with a density of 1,020 kg/m^3 (given by the producer BASF). We randomly selected 30 particles and measured their dimensions using a Vernier caliper, and their fall velocities in a water column. The results show that the sediment characteristics are relatively uniform (Table 1). Based on these measurements, 2.4 mm (cube root of the mean volume) was chosen as the characteristic sediment size; 25 mm/s, as the characteristic fall velocity.

Table 1 Features of the particles

	Minimum value	Mean value	Maximum value
Height (mm)	2.30	2.55	2.85
Major axis (mm)	2.30	2.65	3.00
Minor axis (mm)	1.85	2.10	2.30
Density (kg/m^3)	–	1020 (given by BASF)	–
Fall velocity (mm/s)	20	25	30

2.3 Experimental procedure

After preliminary sediment tests, one single inflow velocity was chosen for all the experiments (0.28 m/s). This velocity was sufficiently high to avoid deposition in the inlet channel and near the entrance of the reservoir (in order to avoid modifications of the direction of the incoming jet), and sufficiently low to allow deposition in the reservoir.

Two kinds of experiments were carried out. The first one consisted in flow tests; their aim was to describe (qualitatively and quantitatively) the flow pattern. The second one consisted in sediment tests; their aim was to describe the spatial distribution of deposits and the trap efficiency of the reservoir. The experimental conditions are given in Table 2 (flow tests) and Table 3 (sediment tests). Here, U = velocity in the inlet channel; ρ = water density; μ = water viscosity; g = gravitational acceleration; u_* = shear velocity; ρ_s = sediment density, d = sediment size; w = sediment fall velocity; and q_s = sediment discharge. The uncertainty was about 0.002 m in the water depth (level meter) and about 0.01 m/s in the velocity

(based on uncertainties in discharge and water depth). The water temperature was between 18 and 20°C, depending on the experiment. In order to check the reproducibility, all the experiments were repeated (except test F15-a for which the flow did not stabilize). Successive tests are named "a", "b", etc.

2.4 Flow tests

Visual investigations employing dye injections disclosed the flow pattern: symmetry or asymmetry, number of circulation zones, approximate locations of reattachment points. Despite steady boundary conditions, a wake zone (characterized by unsteadiness) took place downstream of the entrance of the reservoir. Therefore, successive dye injections were generally needed to describe a "mean" behavior.

The reattachment is defined as the point upstream of which the longitudinal velocity is negative (from downstream to upstream) and downstream of which the longitudinal velocity is positive (from upstream to downstream). Because of the unsteadiness of the flow, Chu et al. (2004) proposed to define it as "the point where the movements to the upstream and downstream directions are equally probable" (this definition corresponds to the median reattachment). To our knowledge, only the median position has been reported in the literature, using for example visualization of displacement of confetti on the water surface (Babarutsi et al., 1989, Babarutsi and Chu, 1991, Chu et al., 2004). Only Abbott and Kline (1962) characterized the fluctuations of the reattachments lengths by taking a large number of points (Figs. 11 and 12 of their paper: the writers showed a band of two regression curves instead of a single one). In the present study, we better characterized these fluctuations by determining the velocity distribution along the wall near the median reattachment. Preliminary tests allowed us to define the following protocol.

Table 2 Summary of flow test conditions and main results ("-" for "non-measured", "Ø" for "does not exist")

Test ID	ΔB (m)	b (m)	L (m)	h (m)	U (m/s)	Flow pattern	R_1 (m) (95% confidence interval)	μ_1 (m)	σ_1 (m)	R_2 (m) (95% confidence interval)	μ_2 (m)	σ_2 (m)
F4-a	0.350	0.285	7.000	0.201	0.28	A2	1.16 – 1.21	1.18	0.10	–	–	–
F4-b	0.350	0.285	7.000	0.200	0.29	A2	1.15 – 1.18	1.16	0.06	–	–	–
F4-c	0.350	0.285	7.000	0.203	0.27	A2	–	–	–	6.0–6.5	6.4	2.1
F14-a	0.350	0.285	2.200	0.205	0.27	A1	1.04 – 1.10	1.07	0.09	Ø	Ø	Ø
F14-b	0.350	0.285	2.200	0.207	0.28	A1	1.03 – 1.06	1.05	0.06	Ø	Ø	Ø
F15-a	0.350	0.285	2.000	0.204	0.27	A1/S0	–	–	–	Ø	Ø	Ø
F16-a	0.350	0.285	1.800	0.206	0.27	S0	Ø	Ø	Ø	Ø	Ø	Ø
F16-b	0.350	0.285	1.800	0.204	0.27	S0	Ø	Ø	Ø	Ø	Ø	Ø

Table 3 Summary of sediment test conditions and main results

Test ID	ΔB (m)	b (m)	L (m)	h (m)	U (m/s)	Flow pattern	C_{in} (g/L)	η_1	η_2	η_3
ST1-a	0.350	0.285	7.000	0.199	0.28	A2	0.50	73%	49%	57%
ST1-b	0.350	0.285	7.000	0.196	0.28	A2	0.50	69%	50%	34%
ST2-a	0.350	0.285	2.200	0.200	0.28	A1	0.50	26%	18%	36%
ST2-b	0.350	0.285	2.200	0.197	0.29	A1	0.50	31%	28%	32%
ST3-a	0.350	0.285	1.800	0.204	0.27	S0	0.51	13%	2%	7%
ST3-b	0.350	0.285	1.800	0.207	0.27	S0	0.50	9%	1%	6%

Once the reattachment had been roughly located by dye visualization, the method consisted in injecting drops of dye at various points against the wall near the reattachment point. In each point, 100 drops of dye were injected at a frequency of one drop every 2 seconds; for each drop, the sense of the flow was observed by eyes. A displacement of the dye from upstream to downstream corresponded to a positive velocity whereas a displacement from downstream to upstream corresponded to a negative velocity. The number of injected drops (100) and the duration of measurement (100 times 2 seconds) were chosen after preliminary tests to ensure a statistically meaningful result. Since the objective of this work is the study of deposits, the reattachment lengths were measured near the bottom of the reservoir (0.04 m above the bed). Nevertheless, "reasonable" two-dimensionality of the flow was always checked by dye visualization.

A 95% confidence interval of the proportion of negative velocities was calculated using a small sample method in order to estimate the "uncertainty" of each measurement (Wonnacott and Wonnacott, 1977). The 95% confidence intervals of the median reattachment lengths were determined using interpolations of the upper-bounds and lower-bounds of the confidence intervals between locations for which the proportions are closest to 50%. The 95% confidence intervals of the median reattachment lengths are given in Table 2 (R_1 and R_2 for respectively the shorter one and the longer one).

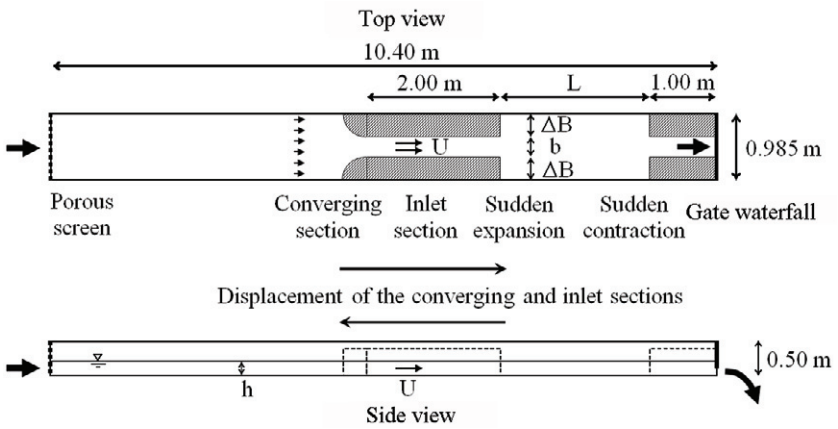

Fig. 2 Sketch of the experimental set-up

Another piece of information was extracted from these measurements: the reattachment lengths fit a normal distribution. By minimizing the sum of the differences between the measured and the normal proportions in square, the mean, μ, and the standard deviation, σ, of a Gaussian distribution were determined. These values are also given in Table 2.

Table 4 summarizes the flow conditions in a dimensionless form. Based on dimensional analysis and literature, six dimensionless flow parameters govern the flow pattern: the dimensionless length (ratio of the length to the lateral expansion), the lateral expansion ratio (ratio of the lateral expansion to the breadth of the inlet channel), the vertical confinement (ratio of the lateral expansion to the water depth), the Reynolds number, the Froude number, and the bed friction number (Table 4). Here, c_f is the bed friction coefficient; it was estimated using the formula recommended by the ASCE task force on friction factor in open channel flow (Henderson, 1966). The bed friction coefficient was used to estimate the shear velocity too. Instead of the lateral expansion ΔB, the breadth B could have been used as the representative lateral dimension of the reservoir.

Table 4 Dimensionless flow parameters

Dimensionless parameter	Value(s)
$\frac{L}{\Delta B}$	5.1, 5.7, 6.3 and 20.0
$\frac{\Delta B}{b}$	1.23
$\frac{\Delta B}{h}$	between 1.69 and 1.78
$\frac{4\rho U h}{\mu}$	between 210,000 and 228,000
$\frac{U}{\sqrt{gh}}$	between 0.19 and 0.21
$\frac{c_f \Delta B}{2h}$	≈ 0.003

In order to allow asymmetric flow patterns to develop in long basins, a lateral expansion ratio greater than 0.25 was chosen (Abbott and Kline, 1962 about "infinitely" long reservoirs). The vertical confinement was chosen sufficiently low to avoid friction effect: the friction had probably no influence on the flow pattern since 0.003 is small compared to the critical values highlighted in the literature (0.05 – 0.10 for unilateral expansions, Chu et al., 2004). The dimensionless lengths were chosen by trial and error in order to find the transition between asymmetric and symmetric flows. Based on preliminary tests about sediment transport (above), a Froude number of 0.20 was chosen. The range of Reynolds numbers shows that the flows were fully turbulent.

2.5 Sediment tests

In order to avoid flocculation, the plastic sediment was wet prior to experiment. It was input into the inflow 2.00 m upstream of the entrance of the reservoir. The injection consisted in discrete batches of 80 g (dry mass) over 10 second time intervals. The total period of injection was 10 minutes for each experiment. The inflow concentration was 0.50 g/L. Based on uncertainties in discharge, sediment mass and time period, the uncertainty in the inflow concentration was about 0.02 g/L.

Using a net, particles were collected in the waterfall downstream of the reservoir in three time periods: between 2 and 4 minutes after the beginning of the injection, between 5 and 7 minutes, and between 8 and 10 minutes. Each sample was dried and weighted, so that the mean outflow concentration could be calculated for the three time intervals. The trap efficiency, η, was calculated for each period using Eq. 1. Here, c_{in} = inflow concentration; c_{out} = outflow concentration.

$$\eta = \frac{c_{in} - c_{out}}{c_{in}} \tag{1}$$

The uncertainty in the outflow concentration was between 0.005 and 0.020 g/L (depending on the outflow concentration), which leads to an absolute uncertainty in the efficiency of 10% – 15% (0.10 – 0.15).

For each experiment, the bed of the reservoir was filmed over time in order to monitor the deposits. The spatial distributions of deposits given below are based on these movies.

Table 5 summarizes the dimensionless sediment parameters: the dimensionless bed shear stress, the particle Reynolds number (calculated with the shear velocity), the dimensionless fall velocity (ratio of the fall velocity to the shear velocity), and the dimensionless solid discharge. Observations by eye showed that bed-load and suspended load coexisted in the inlet channel (the dimensionless fall velocity was about 2). However, bed-load was the predominant mode of transport in the reservoir.

Table 5 Dimensionless sediment parameters

Dimensionless parameter	Value
$\frac{\rho u_*^2}{(\rho_s - \rho) g d}$	≈ 0.3
$\frac{\rho u_* d}{\mu}$	≈ 30
$\frac{w}{u_*}$	≈ 2
$\frac{q_s}{\sqrt{\left(\frac{\rho_s}{\rho} - 1\right) g d^3}}$	≈ 0.5

3 Results

3.1 Flow patterns

Dye visualizations highlighted four different flow patterns. They are reported in Tables 2 and 3.

When the length of the reservoir was 1.80 m, the flow presented a symmetric behavior, as illustrated in Fig. 3 (pattern S0). The jet went in a straight way from the entrance to the exit of the reservoir; two symmetric circulation zones took place in the reservoir. It was also observed that the counter-currents

detached from the wall approximately 0.3 m downstream of the inlet section of the reservoir, leading to the formation of a small circulation zone in each upstream corner. This zone was not drawn as a two-dimensional circulation in Fig. 3 because dye visualization highlighted three-dimensional effects (vertical eddies); this behavior is consistent with the observations of Abbott and Kline (1962).

Symmetry disappeared when increasing the length of the reservoir to 2.20 m. The jet was deflected on one side of the reservoir. It reattached the wall after a distance named R_1 in Fig. 3, which led to the formation of a large circulation zone. A smaller circulation zone took place upstream of the reattachment. This flow pattern is denoted by "A1".

For intermediate length (2.00 m), the flow did not stabilize in spite of steady boundary conditions: it fluctuated between a symmetric behavior (S0) and an asymmetric behavior (A1). The fluctuations between these two patterns were not periodic and seemed to be completely random. This type of flow is reported as "A1/S0" in Table 2. Even if the flow was unsteady in this situation, it was completely different from the meandering jet (periodic behavior) observed by Kantoush (2008) when decreasing the water depth below 0.20 m.

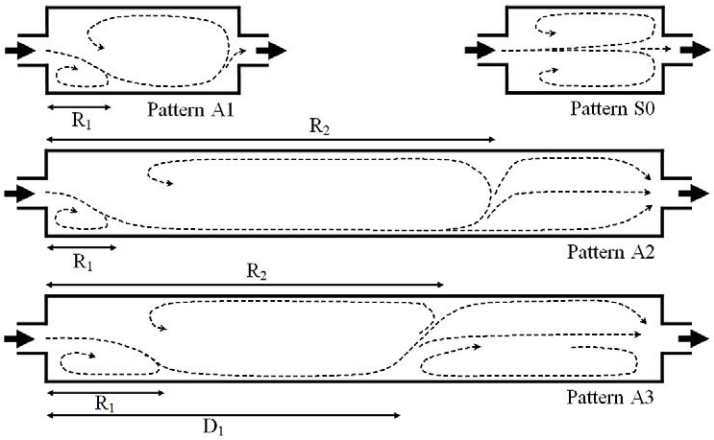

Fig. 3 Schemes of the three stable flow patterns (not to scale)

For the longest reservoir (7.00 m), the flow still remained asymmetric. As for a length of 2.20 m, the flow reattached on one side of the reservoir after a distance R_1 but also possibly on the opposite wall after a distance R_2. In this situation, the flow was fully reattached in the downstream zone of the basin (all the x-velocities in a transversal section are positive). Successive dye visualizations showed that the longer reattachment was highly unsteady, and sometimes completely missing. This third stable pattern is illustrated in Fig. 3 (A2).

These results highlight a transition between symmetric and asymmetric flows for a dimensionless length in the range 5.1 – 6.3 (the flow was symmetric below and asymmetric above). This critical range is different from the results of the experiments carried out by Kantoush (2008) for which the transition occurred for a dimensionless length in the range 2.7 – 3.2. This shows that the dimensionless length is not sufficient to predict the flow pattern; additional dimensionless parameters from Table 4 are needed. There have been several attempts to define a criterion for forecasting the flow pattern in rectangular shallow reservoirs, from the simplest length to breadth ratio (Kantoush, 2007) to more complex criteria involving the length of the reservoir, its breadth (eventually the lateral expansion) and the breadth of the inlet channel (Kantoush, 2008, Dewals et al., 2008, Dufresne, 2008). Among these criteria, only the one defined in Eq. (2) and based on numerical simulations of Dufresne (2008) is consistent with the two experimental campaigns. Indeed, the range corresponding to the transition highlighted by Kantoush (2.2 – 2.6) partially overlaps the range highlighted in the present study (2.3 – 2.9). Moreover, these two ranges are consistent with the critical value that Dufresne (2008) recommended: symmetric flows below 2.36 and asymmetric flows above 2.36.

$$A_L = \frac{L}{B}\left(\frac{B}{b}\right)^{0.2} = \frac{L}{B^{0.8}b^{0.2}} \tag{2}$$

Nevertheless, the relatively close hydraulic conditions of the two campaigns raise the question of the validity of this geometrical criterion in more general situations (various water depths and various velocities). Further investigations varying the lateral expansion ratio, the vertical confinement and the Froude number are currently in progress in order to find a general criterion.

3.2 Reattachment lengths

Figures 4 and 5 display the negative velocity distributions near reattachment for the experimental condition F4 (tests "a" and "c"), which corresponds to the flow pattern A2. Using these figures, the median reattachment length and the range of fluctuation of the reattachment length can be precisely determined. In Table 2, the median reattachment length is given using a 95% confidence interval (measurement uncertainty); the range of fluctuation is given using the mean and the standard deviation of a Gaussian distribution (temporal variability). From Fig. 4, we are for example 95% confident that the median reattachment length R_1 of experiment F4-a was between 1.16 and 1.21 m. Using the normal distribution, one can also extract that the reattachment length was between 1.05 and 1.31 m during 80% of the time; it was smaller than 1.05 m during 10% of the time, and greater than 1.31 m during 10% of the time.

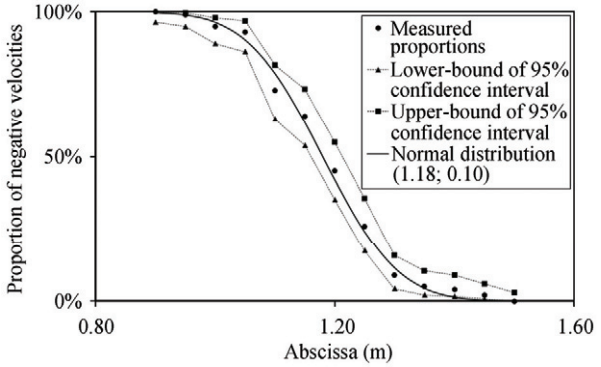

Fig. 4 First reattachment of test F4-a

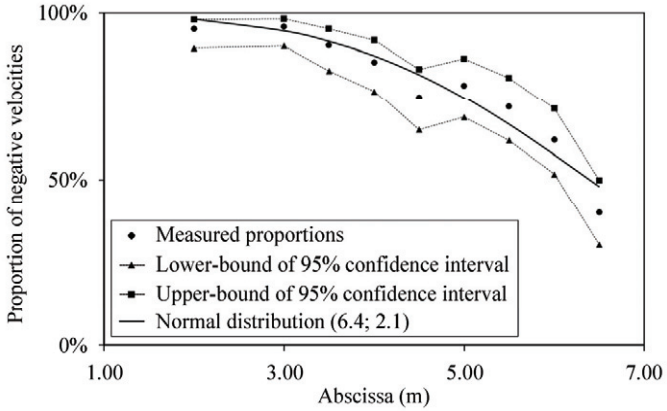

Fig. 5 Second reattachment of test F4-c (the normal distribution is truncated)

The comparison between Figs. 4 and 5 highlights the different nature of the two reattachments. Whereas the first one was rather steady over time (standard deviation about 0.10 m), the second one was highly unsteady (2.1 m), which means that it fluctuated over a long distance on the wall of the reservoir. Here, it must be precised that the distribution of the negative velocities of the second reattachment is not rigorously normal (one can see in Fig. 5 that the distribution of the second reattachment length is truncated by the downstream wall of the reservoir). Nevertheless, we also describe the second reattachment using the mean and the standard deviation of a Gaussian law in order to make possible

comparison between R_1 and R_2. At a distance of 6.5 m from the entrance, the proportion of negative velocities was close to 50%, which means that the reattachment completely disappeared during about half the time (the length of the reservoir is 7.00 m). Therefore, the instantaneous flow fluctuated between A1 and A2 while the median flow was A2, which is consistent with previous dye visualizations (the second reattachment was sometimes missing). The high unsteadiness of the second reattachment length was also highlighted by Abbott and Kline (1962) about flow over backward facing steps.

The median reattachment length R_1 measured for the experimental condition F14 was a little bit smaller than the value measured for F4 (1.04 – 1.10 m and 1.03 – 1.06 m instead of 1.16 – 1.21 m and 1.15 – 1.18 m), which may be interpreted as an effect of the longitudinal confinement. Nevertheless, it can be said that the flow patterns A1 and A2 are quasi-identical in the upstream zone of the reservoir (same order of magnitude for the median position and the variability of the reattachment). They only significantly differ in the downstream zone of the reservoir.

It can be noticed that the median reattachment length of the "last" asymmetric flow before the transition to symmetric pattern was approximately equal to half the length of the reservoir (1.04 – 1.10 and 1.03 – 1.06 m compared to 2.20 m). This behavior was similar in the experiments of Kantoush (2008): the writer showed that when the breadth of the reservoir equaled 4.00 m, the transition occurred between the lengths 5.00 and 6.00 m; the mean reattachment length for a length of 6.00 m was ≈ 2.65 m (Fig. 4.16 of his thesis).

3.3 Spatial distribution of deposits

Figure 6 displays the preferential zones of deposition for the three stable flow patterns after 10 minutes of sediment input (a clear pattern of deposition was observed after 4–5 minutes for all the sediment tests). Since the borders of the deposition zones slightly evolved over time (because of the unsteadiness of the flow), Fig. 6 is only a sketch of the deposits at a given "time" (it is representative of a few seconds). The comparison between grey zones (tests a) and dotted lines (tests b) exhibits the same general shape of deposits.

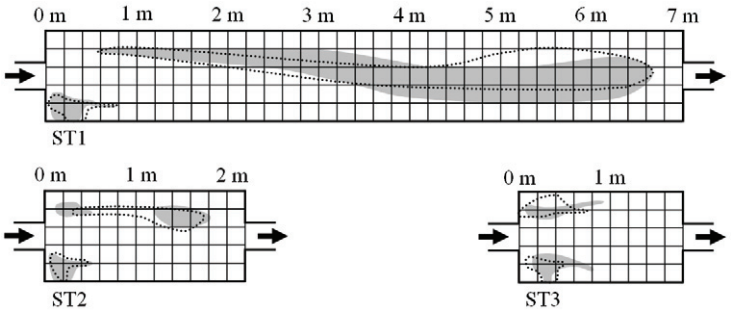

Fig. 6 Experimental deposits on the bed of the reservoir (grey zones correspond to tests a; dotted lines, to tests b)

From this figure, it can be concluded that the location of the deposits is clearly a function of the flow pattern. When the length was 1.80 m (flow pattern S0), the pattern of sediment deposition was quasi-symmetric: deposition took place in each inlet corners. The size of the deposition regions was approximately a few centimeters to 0.3 m in width and 0.4 – 0.8 m in length. The shape of the downstream part of these zones was elongated and corresponded to deposits regularly eroded (wake zone).

Like the flow pattern, the pattern of sediment deposition became asymmetric when increasing the length. When the reservoir was 2.20 m long (flow pattern A1), three regions of deposition took place on the bed: the two inlet corners and the core of the large circulation zone. Here, the jet was deflected on the right wall of the reservoir. Despite its relatively small area (about 0.6 m long and 0.2 m wide), the zone of deposition in the core of the large circulation zone contained the largest amount of deposits. After 10 minutes of injection, the thickness of particles was about 20 mm (several layers of particles) while it was less than 5 mm in the others zones. In this zone, the deposits were regularly eroded due to the relative

unsteadiness of the flow, but they remained captured in the circulation current and escaped only by intermittent "bursts". In the right inlet corner, the region of deposition was about 0.4 m long and 0.2 – 0.3 m wide. As for the 1.80 m long reservoir, the downstream part of this region was regularly eroded because of the wake. The left inlet corner region consisted of very scattered deposits that were brought by the current from downstream to upstream. Regularly, the first and the third regions were connected by a narrow band of (intermittent) deposits (see dotted lines).

When the length was 7.00 m (flow pattern A2), two main zones of deposition were identified. As for the flow pattern A1, a first region took place in the right inlet corner (the jet was deflected to the right). A second region of deposition took place mainly in the downstream zone of the reservoir. Its length was about 6.0 m and its width varied between a few centimeters to approximately 0.4 – 0.6 m in its downstream part. Probably because of the unsteadiness of the flow in this zone (fluctuations of the longer reattachment length), the deposits were regularly eroded. This region of deposition was quasi-symmetric in the downstream part of the reservoir (where the flow was fully reattached). Contrarily to the experimental condition ST2, there was no region of deposition in the left inlet corner of the reservoir. This can be explained by the fact that the current from downstream to upstream that took place in this zone contained a small amount of particles (they settled or escaped before being brought back to the upstream zone of the reservoir).

3.4 Trap efficiency

As shown in Table 3, the efficiencies η_1, η_2 and η_3 (corresponding to the three time periods) are scattered for a given length. Different reasons explain this behavior: the time needed by the particles to travel between the inlet and the outlet (one can see that 2 minutes were not sufficient to get "equilibrium" between the inflow and the outflow concentrations when the length was 7.00 m), the uncertainty of the measurements (10% – 15%), and the natural variability (although the equilibrium is reached, the difference between η_3 obtained for ST1-a and ST1-b is greater than the uncertainty). The first reason leads to reject the η_1 values as meaningful efficiencies for the longest reservoir whereas the η_2 and η_3 values and all the efficiencies obtained for the other lengths are considered hereafter.

The natural variability was probably due to the unsteadiness of the flow, the unsteadiness of the sediment input (discrete batches) and also the nature of sediment transport itself, especially because bed-load was predominant. Indeed, Böhm et al. (2004) showed that even under well-controlled experimental conditions and despite steady supply, solid discharge exhibits significant variations with time. One explanation given by the writers was the collective entrainment of deposited particles, which was observed during our own experiments. This physical variability leads to define some ranges of efficiency rather than single values. Table 6 shows these approximate ranges as a function of the length of the reservoir. In this table, both uncertainty and variability are taken into account.

Table 6 Ranges of trap efficiencies varying the length of the reservoir

Length (m)	Trap efficiency
1.80	0% – 20%
2.20	10% – 40%
7.00	30% – 60%

The influence of the length of the reservoir on the efficiency is illustrated in Fig. 7. It can be seen that the decrease of the efficiency between 2.20 and 1.80 m is the same order of magnitude as the decrease between 7.00 and 2.20 m (about 20% – 25%). Therefore, the transition from an asymmetric flow to a symmetric flow is responsible for a break in the efficiency curve of the reservoir.

Even if the flow patterns observed for a length of 7.00 m and a length of 2.20 m were very similar, it is interesting to notice that the nature of deposition seemed to be different, probably because the particles were jailed in the circulation current for experiments ST2-a and ST2-b. Based on the sketches of the experimental deposits (Fig. 6), the areas of deposition were estimated. Whereas the area of deposition was about 0.3 m^2 for a length of 2.20 m, it was around 1.9 m^2 (six times bigger) for a length of 7.00 m. In the same time, the efficiency only increases from the range 10% – 40% to 30% – 60%. One explanation is that the particles are concentrated in the center of the circulation zone for the flow pattern A1 (as "jailed" by the flow) whereas they are much dispersed for the flow pattern A2.

Although the number of points is too low and the values too scattered to propose a final relationship between the length of the reservoir and the efficiency, assumptions can be made and discussion is open. To do so, it can be added that the efficiency should tend towards zero when decreasing the length. But the efficiency does not necessarily tend towards 100% when increasing the length (even if it is fully reattached, the flow may be able to carry a non-zero solid discharge because of the relatively small breadth of the flume).

Exponential laws were often proposed as efficiency relationships (Sumer 1977 cited by Garde et al., 1990, Garde et al., 1990, Ranga Raju and Kothyari, 2004 for settling basins; Luyckx et al., 1999 for the parameters of the efficiency relationship of a high side weir overflow). In this study, contrarily to the cited relationships, the constant L_0 of such a law (Eq. 3) must be different from zero to accurately reproduce the abrupt change around the transition; this parameter is the length for which the efficiency becomes zero. The two other constants are η_0, a maximum efficiency (for infinitely long reservoir) and α, the inverse of a characteristic length (to represent the spread of the curve). This exponential relationship leads to negative values when the length is lower than L_0; therefore, the expression is replaced by zero in this situation.

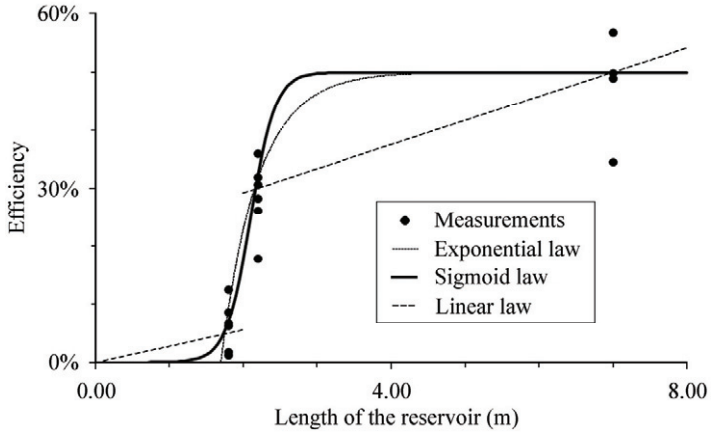

Fig. 7 Trap efficiency as a function of the length of the reservoir (parameters of the exponential law: $\eta_0 = 50\%$, $\alpha = 2$ m^{-1}, $L_0 = 1.7$ m; sigmoid law: $\eta_0 = 50\%$, $\alpha = 6$ m^{-1}, $L_0 = 2.1$ m)

$$\begin{aligned} \eta &= 0\% \quad \text{if } L \le L_0 \\ \eta &= \eta_0\left(1 - e^{-\alpha(L-L_0)}\right) \quad \text{if } L \ge L_0 \end{aligned} \tag{3}$$

The inconvenience of such a law is that the constant L_0 has no meaning in relation to the flow pattern. A sigmoid law (as written in Eq. 4) is more relevant to highlight the transition between symmetric and asymmetric flows in the efficiency relationship. Here, the constants of the law are a maximum efficiency, η_0, the inverse of a characteristic length, α, and a critical length, L_0. This last parameter is the length for which the transition between asymmetry and symmetry occurs and is therefore between 1.80 and 2.20 m.

$$\eta = \frac{\eta_0}{1 + e^{-\alpha(L-L_0)}} \tag{4}$$

The exponential law, the sigmoid law and two linear relationships (comparable slopes but different intercept points) are illustrated in Fig. 7; all of them reproduce the general shape of the experimental data.

The laws described above are some possibilities for taking into account the transition between symmetric and asymmetric flow patterns in a single efficiency relationship, but it is perhaps unrealistic to seek such a goal. In this case, the only way would be to use different regression laws depending of the flow pattern.

4 Conclusions

The objective of this work was to investigate the influence of the flow pattern on preferential regions of deposition and trap efficiency in rectangular shallow reservoirs. The great flexibility of the experimental

set-up allowed easily changing the length of the reservoir and precisely determining the transition between symmetric and asymmetric flow patterns.

Four flow patterns were identified (from longer to shorter reservoirs): an asymmetric flow with two reattachment points (A2), an asymmetric flow with one reattachment point (A1), an unstable flow (A1/S0), and a symmetric flow without any reattachment point (S0). Using dye visualizations, the median value and the temporal variability of the reattachment lengths were precisely measured for the asymmetric flow patterns A1 and A2.

For each stable flow, sediment tests with plastic particles were carried out. The regions of deposition on the bed of the reservoir were mapped; they were clearly a function of the flow pattern. The transition between symmetric to asymmetric flow patterns was responsible for an abrupt increase in the efficiency curve. We discussed a number of regression laws to take it into account.

Further investigations are currently in progress in order to find forecasting criteria of the flow pattern varying the dimensionless length, the lateral expansion ratio, the vertical confinement and the Froude number. Based on this work, the data about trap efficiency available in literature should be reanalyzed in order to better define efficiency relationships.

Acknowledgements

We acknowledge Alain Dewart, Didier Lallemand, Maurice Salme and Dieudonné Stouvenakers for the building of the experimental set-up. We also acknowledge the University of Liège for the allocation of a postdoctoral fellowship to the first author.

References

Abbott D. E. and Kline S. J. 1962, Experimental investigation of subsonic turbulent flow over single and double backward facing steps. Journal of Basic Engineering, Vol. 84, pp. 317–325.

Babarutsi S. and Chu V. H. 1991, Dye-concentration distribution in shallow recirculating flows. Journal of Hydraulic Engineering, Vol. 117, No. 5, pp. 643–659.

Babarutsi S., Ganoulis J., and Chu V. H. 1989, Experimental investigation of shallow recirculating flows. Journal of Hydraulic Engineering, Vol. 115, No. 7, pp. 906–924.

Böhm T., Ancey C., Frey P., Reboud J.-L., and Ducottet C. 2004, Fluctuations of the solid discharge of gravity-driven particle flows in a turbulent stream. Physical Review E, Vol. 69, No. 6, pp. 061307:1–13.

Chu V. H., Liu F., and Altai W. 2004, Friction and confinement effects on a shallow recirculating flow. Journal of Environmental Engineering and Science, Vol. 3, pp. 463–475.

Dewals B. J., Kantoush S. A., Erpicum S., Pirotton M., and Schleiss A. J. 2008, Experimental and numerical analysis of flow instabilities in rectangular shallow basins. Environmental Fluid Mechanics, Vol. 8, pp. 31–54.

Dufresne M. 2008, La modélisation 3D du transport solide dans les bassins en assainissement: Du pilote expérimental à l'ouvrage réel. PhD thesis, Université Louis Pasteur, Strasbourg, France (in French).

Dufresne M., Vazquez J., Terfous A., Ghenaim A., and Poulet J.-B. 2009, Experimental investigation and CFD modelling of flow, sedimentation, and solids separation in a combined sewer detention tank. Computers & Fluids, Vol. 38, No. 5, pp. 1042–1049.

Garde R. J., Ranga Raju K. G., and Sujudi A. W. R. 1990, Design of settling basins. Journal of Hydraulic Research, Vol. 28, No. 1, pp. 81–91.

Henderson F. M. 1966, Open channel flow, Macmillan Series in Civil Engineering, Prentice Hall.

Jothiprakash V. and Garg V. 2008, Re-look to conventional techniques for trapping efficiency estimation of a reservoir. International Journal of Sediment Research, Vol. 23, No. 1, pp. 76–84.

Kantoush S. A., Bollaert E., and Schleiss A. J. 2008, Experimental and numerical modelling of sedimentation in a rectangular shallow basin. International Journal of Sediment Research, Vol. 23, No. 3, pp. 212–232.

Kantoush S. A. 2008, Experimental study on the influence of the geometry of shallow reservoirs on flow patterns and sedimentation by suspended sediments. PhD thesis, Ecole Polytechnique Fédérale de Lausanne, Switzerland.

Kantoush S. A. 2007, Symmetric or asymmetric flow patterns in shallow rectangular basins with sediment transport. Proceedings of the 32nd Congress of IAHR, "Harmonizing the Demands of Art and Nature in Hydraulics", Venice, Italy.

Kowalski R., Reuber J. and Köngeter J. 1999, Investigations into and optimisation of the performance of sewage detention tanks during storm rainfall events. Water Science and Technology, Vol. 39, No. 2, pp. 43–52.

Luyckx G., Vaes G., and Berlamont J. 1999, Experimental investigation on the efficiency of a high side weir overflow. Water Science and Technology, Vol. 39, No. 2, pp. 61–68.

Ranga Raju K. G. and Kothyari U. C. 2004, Sediment management in hydroelectric projects. Proceedings of the 9th International Symposium on River Sedimentation, Yichang, China.

Ranga Raju K. G., Kothyari U. C., Srivastav S., and Saxena M. 1999, Sediment removal efficiency of settling basins. Journal of Irrigation and Drainage Engineering, Vol. 125, No. 5, pp. 308–314.
Saul A. and Ellis D. 1992, Sediment deposition in storage tanks. Water Science and Technology, Vol. 25, No. 8, pp. 189–198.
Stovin V. R. 1996, The prediction of sediment deposition in storage chambers base on laboratory observations and numerical simulation. PhD thesis, University of Sheffield, United Kingdom.
Stovin V. R. and Saul A. J. 1996, Efficiency prediction for storage chambers using computational fluid dynamics. Water Science and Technology, Vol. 33, No. 9, pp. 163–170.
Stovin V. R. and Saul A. J. 1994, Sedimentation in storage tank structures. Water Science and Technology, Vol. 29, No. 1-2, pp. 363–372.
Sumer B. 1977, Settlement of solid particles in open-channel flow. Journal of the Hydraulics Division, Vol. 103, No. 11, pp. 1323–1337.
Wonnacott T. and Wonnacott R. 1977, Introductory Statistics, Third edition, John Wiley and Sons.